Open Access Articles

Ecosystem respiration increases with biofilm growth and bed forms: Flume measurements with resazurin

The Faculty of Oregon State University has made this article openly available.
Please share how this access benefits you. Your story matters.

Citation	Haggerty, R., Ribot, M., Singer, G. A., Martí, E., Argerich, A., Agell, G., & Battin, T. J. (2014). Ecosystem respiration increases with biofilm growth and bed forms: Flume measurements with resazurin. Journal of Geophysical Research: Biogeosciences, 119(12), 2220-2230. doi:10.1002/2013JG002498
DOI	10.1002/2013JG002498
Publisher	American Geophysical Union
Version	Version of Record
Terms of Use	http://cdss.library.oregonstate.edu/sa-termsofuse

Oregon State
UNIVERSITY OSU

Correspondence to:
R. Haggerty,
haggertr@geo.oregonstate.edu

Ecosystem respiration increases with biofilm growth and bed forms: Flume measurements with resazurin

Roy Haggerty[1], Miquel Ribot[2], Gabriel A. Singer[3,4], Eugènia Martí[2], Alba Argerich[5], Gemma Agell[2], and Tom J. Battin[3,6]

[1]College of Earth, Oceanic, and Atmospheric Sciences, Oregon State University, Corvallis, Oregon, USA, [2]Biogeodynamics and Biodiversity Group, Centre d'Estudis Avançats de Blanes (CSIC), Blanes, Spain, [3]WasserCluster Lunz Biologische Station GmbH, Lunz, Austria, [4]Leibniz-Institute of Freshwater Ecology and Inland Fisheries (IGB), Berlin, Germany, [5]Department of Forest Ecosystems and Society, Oregon State University, Corvallis, Oregon, USA, [6]Department of Limnology, University of Vienna Wien, Vienna, Austria

Abstract In a set of streamside mesocosms, stream ecosystem respiration (*ER*) increased with biofilm biomass and flow heterogeneity (turbulence) generated by impermeable bed forms, even though those bed forms had no hyporheic exchange. Two streamside flumes with gravel beds (single layer of gravel) were operated in parallel. The first flume had no bed forms, and the second flume had 10 cm high dune-shaped bed forms with a wavelength of 1.0 m. Ecosystem respiration was measured via resazurin reduction to resorufin in each flume at three different biomass stages during biofilm growth. Results support the hypothesis that *ER* increases with flow heterogeneity generated by bed forms across all biofilm biomass stages. For the same biofilm biomass, *ER* was up to 1.9 times larger for a flume with 10 cm high impermeable bed forms than for a flume without the bed forms. Further, the amount of increase in *ER* associated with impermeable bed forms was itself increased as biofilms grew. Regardless of bed forms, biofilms increased transient storage by a factor of approximately 4.

1. Introduction

Stream ecosystem respiration (*ER*) is one of the most important processes in streams, influencing most chemical conditions (e.g., dissolved oxygen, pH, and dissolved organic carbon) and most other reactions (e.g., denitrification) in streams. *ER* is an important indicator of stream ecosystem function and structure [*Bernot et al.,* 2010], and *ER* is significantly correlated to nutrient uptake in many systems [*Mulholland et al.,* 2009; *Hoellein et al.,* 2007]. In addition to its local importance, *ER* accounts for a major, though poorly constrained fraction of global terrestrial net CO_2 release to the atmosphere [*Battin et al.,* 2009; *Cole et al.,* 2007; *Tranvik et al.,* 2009]. While many of the first-order relationships have been identified, *ER* is not yet sufficiently well understood to allow local measurements to be upscaled to regional, letalone global, estimates of either carbon or nutrient cycling.

Most stream *ER* occurs in biofilms in stream beds [*Fuss and Smock*, 1996; *Naegeli and Uehlinger*, 1997] where the microbial assemblages are protected from wash out [*Battin et al.,* 2009]. We also know that *ER* is controlled by temperature [*Sinsabaugh*, 1997; *Acuña et al.,* 2004; *Demars et al.,* 2011; *Perkins et al.,* 2012] and that the change in respiration with temperature is well described by the Arrhenius equation [*Yvon-Durocher et al.,* 2012]. We know that *ER* is controlled by the standing crop of biomass [*Jones et al.,* 1995; *Cardinale et al.,* 2002; *Acuña et al.,* 2004], sometimes made more labile by disturbance [*Jones et al.,* 1995; *O'Connor et al.,* 2012]. Nutrients influence *ER* because they may increase autotrophic and heterotrophic metabolism [*Mulholland et al.,* 2001; *Hoellein et al.,* 2007; *Bernot et al.,* 2010]. Hydrodynamics at the water-sediment interface influence respiration [e.g., *O'Connor and Hondzo*, 2008; *O'Connor et al.,* 2009; *Inoue and Nakamura*, 2011] because hydrodynamics control the transport of oxygen, nutrients, and waste products to and from the respiration sites. The amount and rate of transient storage may influence *ER* [*Jones et al.,* 1995; *Mulholland et al.,* 1997; *Fellows et al.,* 2001; *Ingendahl et al.,* 2009; *Bernot et al.,* 2010], but this relationship seems less general and work remains to understand it.

We also have evidence that turbulence increases *ER* [*Cardinale et al.,* 2002; *Singer et al.,* 2010]. Turbulence may increase solute exchange between the water column and streambed. Increased solute exchange may

deliver more substrate and more oxygen, and carry away waste products. If biofilms are not disrupted, the transport may increase microbial activity and, ultimately, ER in streams. Cardinale et al. [2002] showed that ER increased with physical heterogeneity of the streambed and hypothesized that this was due to increased turbulence intensity caused by the heterogeneity. Singer et al. [2010] further showed that DOC uptake in biofilms increased with flow heterogeneity (measured as standard deviation over space of the magnitude of water velocity) and turbulence intensity, which could lead to increased biofilm respiration rates. The causal link in the relationship between increased flow heterogeneity and increased ER is not yet understood. In particular, we do not yet know if increased ER is a purely physical response, or if there is a biological response to flow heterogeneity that is also involved. Furthermore, ER is challenging to measure accurately in most streams because reaeration dominates the oxygen budget. Therefore, more data are needed relating ER to flow heterogeneity.

In this study, we tested the hypothesis that ER increases with flow heterogeneity caused by boundary roughness, and that this increase holds across a range of biofilm conditions. We wanted to separate effects at the interface between the stream and bed from the effects of hyporheic exchange within the bed, both of which are associated with ER. The test was done with the smart tracer, resazurin. Resazurin (Raz) is a metabolically active compound that reacts irreversibly to resorufin (Rru) [Haggerty et al., 2008, 2009; Argerich et al., 2011]. The rate of the Raz-to-Rru reaction provides a measure of net aerobic respiration [González-Pinzón et al., 2012]. Since Raz does not exist in streams, and is not subject to reaeration, changes in ER due to processes such as turbulence can be measured more accurately.

2. Methods

2.1. Flumes

The study lasted 45 days and was conducted in two streamside flumes (40.0 m length and 0.40 m width). These are the same flumes as used by Bottacin-Busolin et al. [2009] and Singer et al. [2010]. One flume had a completely flat bed (hereafter "planform"), and the second flume contained 38 triangular dune-shaped bed forms of 10 cm height and 1 m wavelength (hereafter "bed form"). These impermeable flume beds were covered with a single layer of clean, manually scrubbed gravel (median diameter = 9.2 mm, all diameters <40 mm) excavated from the nearby stream as substrate for biofilm growth. The bed form flume had 2.3% more gravel than the planform flume because the bed forms generated 2 – 3% more surface area. Flumes received identical raw stream water [Oberer Seebach, Austria; see Battin, 1999 and references therein for biogeochemical description] with a discharge of 2.25 L s^{-1} that was held steady by directing the supply water through a header tank fitted with an overflow. Flows were checked daily. Tilting weirs at the flume ends generated flow that was spatially uniform at scales larger than the bed form wavelength. The mean velocities in the flumes were made similar by adjusting flume slope in conjunction with measurements of mean velocity by slug additions of NaCl solution [Gordon et al., 2004; Stream Solute Workshop (SSW), 1990]. Slopes were 0.01% for the planform flume and 0.3% for the bed form flume. Except during times of experimental tracer additions, the flumes were fed in a once-through mode to provide identical microbial inocula and aqueous chemical conditions. During experiments, water was recirculated individually through both flumes with discharge equal to the once-through mode.

Periodically measured outflow concentrations of $NO_3^- + NO_2^-$ averaged $1119 \pm 20 \, \mu gN \, L^{-1}$ (mean ± standard error), NH_4^+ averaged $6.14 \pm 0.95 \, \mu gN \, L^{-1}$, and PO_4^{2+} averaged $1.77 \pm 0.44 \, \mu gN \, L^{-1}$. Water temperature averaged $8.7 \pm 0.4°C$.

Ecosystem respiration and turbulence were measured under three different biofilm development conditions: after 0, 11, and 30 days of growth (minimum, medium, and maximum biofilm growth, respectively). At 0 days, the gravel was scrubbed manually until visually clean. However, a small amount of biofilm would have been present.

2.2. Flow Heterogeneity and Turbulence

We described flow heterogeneity and turbulence using 3-D velocity data collected with an acoustic Doppler velocimeter (ADV; Vectrino® Nortek, 4-beam side-looking probe, 50 Hz for 1 min, time series of $n = 3000$). In each flume, velocity was mapped over one bed form wavelength: (i) vertically along the thalweg in the xz plane and (ii) horizontally above the sediment surface (~5 mm above the tops of the grains). The detailed
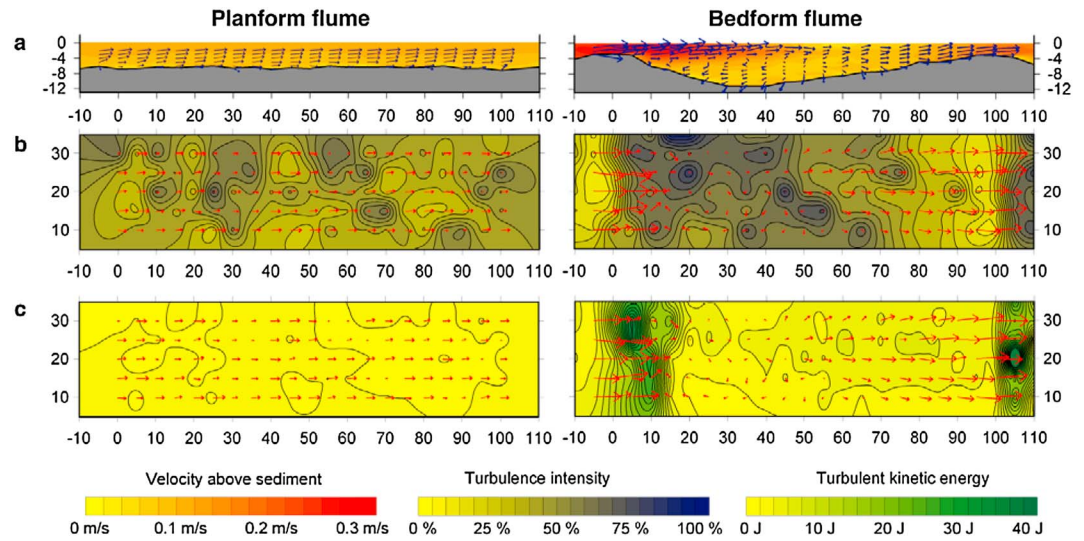
Figure 1. Characterization of flow spatial variability in the planform and bed form flumes based on acoustic Doppler velocimetry measurements. (a) 120 cm long vertical sections along the thalweg show velocity conditions in the XZ plane. Arrows are *x-z* components of the 3D velocity vector; arrow length is proportional to temporally averaged velocity (means of velocity time series with $n = 3000$ at each location). Background colors indicate velocity. Filled contours were created from Kriging-interpolated data for display only. Grey area is a single layer of natural gravel (<40 mm) covering an impermeable flume bed. All axis distances in cm. An individual bed form starts at $x = 0$ cm and ends at $x = 100$ cm. (b) Turbulence intensity (shown as filled contours based on Kriging-interpolated values) and *x-y* components of the velocity vector of the near-substratum measurement as arrows. (c) Turbulent kinetic energy (filled contours, Kriging-interpolated) with identical velocity arrows as in Figure 1b. The same scaling was used for the continuous color representations and the arrows for bed form and planform flume.

vertical profiles (1 and 5 cm vertical and horitzontal spacing, respectively) were only used for graphical representation of the flow fields (Figure 1). The horizontal measurements resulted in a 5×5 cm grid evenly covering an entire bed form with 80 nodes, for which we calculated (i) the mean of the three-dimensional velocity vector $\overline{R}_{xyz}$ (as a temporal mean from the time series with $n = 3000$, hereafter "mean velocity"), (ii) turbulent kinetic energy per unit volume (TKE), and (iii) turbulence intensity TI. $\overline{R}_{xyz}$, TKE, and TI are computed according to *Bradshaw* [1971] and *Gordon et al.* [2004]:

$$\overline{R}_{xyz} = \frac{\sum_{i=1}^{n=3000} \sqrt{u_i^2 + v_i^2 + w_i^2}}{n}, \tag{1}$$

where u_i, v_i, and w_i are the three orthogonal velocity components of ADV data point *i*,

$$TKE = \frac{1}{2}\rho\left(u'^2 + v'^2 + w'^2\right), \tag{2}$$

where u', v', and w' are the mean deviations from the associated mean orthogonal velocity components, ρ is the density of water, and

$$TI = \frac{tSD_{Rxyz}}{\overline{R}_{xyz}}, \tag{3}$$

where $tSD_{R_{xyz}}$ is the temporal standard deviation of the 3-D velocity time series ($n = 3000$ measurements) at each of the 80 locations. TI is a measure of turbulence standardized for mean velocity, while TKE includes the kinetic energy of mean velocity and turbulence; both describe the fluctuating hydrodynamic environment experienced by the benthic biota. Shear velocity *u** was computed from *TKE* as:

$$u* = 0.37\sqrt{\frac{TKE}{\rho}} \tag{4}$$

where TKE/ρ is turbulent kinetic energy per unit mass [*Dade et al.*, 2001]. Due to the wake flow developed downstream of bed forms, shear could not be estimated from vertical profiles of velocity. Last, we computed $SD_{\bar{R}_{xyz}}$, the standard deviation of the mean velocity $\bar{R}_{xyz}$ over the 80 locations, which is a measure of flow heterogeneity at the flume scale. In contrast to $tSD_{R_{xyz}}$, $SD_{\bar{R}_{xyz}}$ describes the spatial variation of flow velocity and is computed from temporal means. The depth-based Reynolds number and Froude number were calculated according to the standard equations [e.g., *Gordon et al.*, 2004]. All raw velocity data were automatically processed and subjected to a filtering procedure using a batch-processing code set up in the statistical language R version 2.7.1 [*R-Development-Core-Team,* 2010]. Filtering removed outliers which were due to low particle concentration in the stream water causing an unreliable ADV-signal. Outliers were identified from the first time derivative of each velocity component as large changes in velocity within short times. Outliers were removed if the first derivative was more than five standard deviations from its mean. To avoid the standard deviation itself being influenced by outliers, the standard deviation was estimated from the range between the 16 and 84 percentiles divided by two, which is the standard deviation of a normal distribution. Outliers were excluded rather than interpolated. The number of excluded outliers was $0.004 +/- 0.007\%$ (mean $\pm$ SD) of all values in each data set, and it was always $<0.1\%$ of values. For the purpose of display in Figure 1, continuous distributions of velocity and derived variables were computed by Kriging using the software Surfer v.8.0 (Golden Software Inc., Colorado, USA) and a 2 mm interpolation grid.

2.3. Measurement of Ecosystem Respiration and Biofilm Biomass

We performed three coinjections of a conservative tracer (NaCl) and Raz in order to estimate transport parameters (velocity, dispersion, and exchange parameters) and respiration rates under the three different biofilm development conditions (days 0, 11, and 30). The three tracer additions were completed between 17 July and 18 August 2008. A 21.6 L solution containing 3.0 kg NaCl as a conservative tracer and 8.503 g Raz was released into the flumes at a rate of $0.817 \pm 0.024\,\mathrm{mL\,s^{-1}}$ for 40 min while the flumes were run in once-through mode (no recirculation). After reaching plateau conditions (steady state concentration of solute at the downstream end of the flume), we turned the solute addition off, switched the flumes to recirculation flow, and allowed 3 to 5 h of reaction time between the Raz/Rru tracer system and biofilm. Conductivity was recorded automatically every 10 s at the end of the flume using a WTW 340i portable conductivity meter (Weilheim, Germany) connected to a CR800 Campbell Scientific data logger (Logan, Utah, USA).

We sampled water for Raz and Rru at the end of the flumes every 30 min. Additionally, we monitored photoreactivity with $174.8\,\mu\mathrm{g\,L^{-1}}$ Raz and $22\,\mu\mathrm{g\,L^{-1}}$ Rru standards. One standard set was placed in the dark, and another set was placed in ambient light next to the flumes. Standard samples were collected every 2 h until the end of each experiment. All samples were immediately filtered through Whatman (Kent, UK) GF/F glass fiber filters ($0.7\,\mu\mathrm{m}$ pore size), placed in acid-washed glass scintillation vials and stored on ice in the dark until laboratory analysis within 12 h.

At the laboratory, samples were buffered to pH 8 [*Haggerty et al.*, 2008] before measurement of fluorescence of Raz and Rru on a Hitachi F-7000 spectrofluorometer (Hitachi High Technologies America, USA). Excitation and emission wavelengths for Raz were 602 and 630 nm, respectively, and for Rru were 570 and 583 nm, respectively.

In order to track biofilm biomass changes over time, glass slides were placed in the flumes at the beginning of the experiments. Slides were placed on the gravel surface at 9, 19, and 32 m from the top of the flume in the planform flume and at the top and the bottom of the crests in the bed form flume. Slides were collected after 11 and 30 days ($n = 3$ slides per day of collection in the planform flume; $n = 3$ slides at the crest $+3$ slides at the bottom per day of collection at the bed form flume). Biofilm on slides was scraped into a known water volume and filtered through Whatman (Kent, United Kingdom) GF/F glass fiber filters ($0.7\,\mu\mathrm{m}$ pore size). Filters were oven-dried at 60°C for 24 h, weighed on a Sartorius MC1 analytical balance (Göttingen, Germany), and combusted at 500°C for 5 h to estimate ash-free dry mass (AFDM).

2.4. Model to Estimate Raz-Rru Transformation Rates

For reactive solutes such as Raz and Rru, the following equations describe transport and transformation for the flumes [simplified from *Argerich et al.*, 2011]. Equations (5)–(6) simplify to the transient storage equations

[*Bencala and Walters*, 1983] if the reaction rates for Raz and Rru are set to zero and retardation factors are set to one.

$$\frac{\partial C_{Raz}}{\partial t} = -\frac{Q}{A}\frac{\partial C_{Raz}}{\partial x} + \frac{1}{A}\frac{\partial}{\partial x}\left(AD\frac{\partial C_{Raz}}{\partial x}\right) - \frac{A_s}{A}\alpha_2[C_{Raz} - S_{Raz}] \tag{5}$$

$$R_{Raz}\frac{\partial S_{Raz}}{\partial t} = \alpha_2(C_{Raz} - S_{Raz}) - (k_{12} + k_1)S_{Raz} \tag{6}$$

$$\frac{\partial C_{Rru}}{\partial t} = -\frac{Q}{A}\frac{\partial C_{Rru}}{\partial x} + \frac{1}{A}\frac{\partial}{\partial x}\left(AD\frac{\partial C_{Rru}}{\partial x}\right) - \frac{A_s}{A}\alpha_2[C_{Rru} - S_{Rru}] \tag{7}$$

$$R_{Rru}\frac{\partial S_{Rru}}{\partial t} = \alpha_2(C_{Rru} - S_{Rru}) - k_2 S_{Rru} + (k_{12} + k_1)S_{Raz} \tag{8}$$

In these equations, concentrations of Raz and Rru are indicated by subscripts, C is the concentration in the flowing water (mol L^{-1}), S is the concentration in transient storage (mol L^{-1}), R_{Raz} and R_{Rru} are retardation factors associated with sorption of Raz and Rru (−), Q is discharge (L s^{-1}), A is the cross-sectional area of the stream (m^2) calculated from discharge and velocity where velocity is estimated by salt arrival, A_s is the cross-sectional area of the transient storage zone (m^2), and D is the dispersion coefficient (m^2 h^{-1}). Further, α_2 is the first-order rate coefficient for solute exchange between the stream and the storage zone, which is equal to the inverse of the mean residence time in the storage zone and equal to $\alpha A/A_s$, where α is the storage zone exchange coefficient of *Bencala and Walters* [1983] and others [e.g., *Runkel*, 1998] (h^{-1}). Last, k_{12} is the Raz to Rru transformation rate coefficient (h^{-1}), k_1 is the Raz decay rate coefficient (h^{-1}), and k_2 is the Rru decay rate coefficient (h^{-1}). Here, the decay rate coefficients k_1 and k_2 can be thought of as loss to unquantified process. The equations assume that (a) all reaction happens within biofilms, which we model as a transient storage zone with an exponential residence time distribution [*Battin et al.*, 2003; *Bottacin-Busolin et al.*, 2009] and (b) sorption happens only within the transient storage zone, although results will be insensitive to any assumptions about sorption. Initial conditions were zero concentrations of Raz, Rru, and NaCl. The upstream boundary was constant injection for 40 min. During the throughflow, the downstream boundary was placed at infinity, and concentrations were modeled at $x = L = 40.0$ m.

The full equations were solved with a version of STAMMT-L [*Haggerty and Reeves*, 2002] for the first 40 min of transport with NaCl, which was the period of the experiments when the flumes were run in once-through mode. The NaCl model was used to estimate D and A_s/A based on measured specific conductivities rather than actual NaCl concentrations. This assumes that the storage zone measured by the conservative tracer is exactly the same as the region where Raz is exchanged, but this is probably not the case because Raz is consumed within the biofilm.

Raz-to-Rru transformation rates were calculated with the simple method described by *Haggerty* [2013] in which equations (5)–(8) have the following solution at steady state and with a typical dispersion rate:

$$\ln\left(\frac{C_{Rru}}{C_{Raz}} + P\right) = \tau\frac{A_s}{A}k_{12} + \ln\left(\frac{C_{Rru,0}}{C_{Raz,0}} + P\right) \tag{9}$$

where τ is the reaction time since the initial concentrations (h). In our flumes, the reaction time is time since flume recirculation started and the injection was stopped. P is the production-decay ratio (−) [see *Haggerty*, 2013, particularly equation (22) and following], and includes effects of irreversible sorption, photodecay, and any other mass losses. While P was unknown, other experiments have shown it to be 0.3 to 0.8 [*Haggerty*, 2013]. We set it to 1 and performed a sensitivity analysis, which we consider in the discussion. $C_{Rru,0}$ and $C_{Raz,0}$ are concentrations (mol L^{-1}) when the flume recirculation started and injection was stopped. The value $\ln\left(\frac{C_{Rru,0}}{C_{Raz,0}} + P\right)$ is, of course, the *y*-intercept at $\tau = 0$.

2.5. Estimation of Ecosystem Respiration (*ER*)

We used the uptake rate, $v_f = \frac{A_s}{A}k_{12}d$ as a proxy for *ER*. We calculated v_f with the slope of equation (9), $\frac{A_s}{A}k_{12}$, multiplied by the effective water depth, d. The value of $\frac{A_s}{A}k_{12}$ was calculated for each experiment ($n = 6$, two flumes at days 0, 11, and 30) from linear regression to plots of $\ln\left(\frac{C_{Rru}}{C_{Raz}} + 1\right)$. The value of d was calculated for each experiment from the known disharge (Q), the velocity calculated from the conservative tracer experiment, and the channel width. We estimate that the uncertainty in d is approximately 10%. The uptake

Table 1. Comparison Velocity, Hydrodynamics, and Turbulence Measurements Between Planform and Bed Form Flumes[a]

	Planform Flume		Bed Form Flume	
	Mean	SD	Mean	SD
Velocity, R_{xyz} (m h^{-1})	283	58	454	226
Shear velocity, $u*$ (m h^{-1})	59	10	99	44
TKE (J m^{-3})	2.0	0.6	6.6	7.1
TI (%)	42	11	50	17

[a]Acoustic Dopper velocimetry (ADV) was used to measure 3D velocity at 80 locations regularly distributed in a 5×5 cm grid over one entire bed form (100 cm flume length) for each flume type. Reported means and standard deviations (SD) describe spatial averages and variations, i.e., they are computed from temporally averaged data. Temporal average velocities, shear velocities, TKE, and TI were computed from the entire ADV time series ($n = 3000$) at each of the 80 locations.

velocity is widely used in stream ecology to normalize reaction rates for velocity and depth [*SSW*, 1990; *O'Connor*, 1988] so values can be compared across experiments with different hydrologic conditions. The v_f of Raz is the net mass flux per unit concentration in the water column and can be thought of as the effective velocity of removal. It is proportional to v_f of oxygen. We did not have dissolved oxygen or gas exchange data for the flume experiments, and so we did not calculate ecosystem respiration values independently. *González-Pinzón et al.* [2012] showed that Raz-Rru reaction rates were proportional to *ER* from dissolved oxygen mass balance. Therefore, for the purpose of this study, comparison of v_f across the experiments is a valid approach to test the effects of biomass and bed forms on biofilm respiration.

2.6. Statistical Analyses

We examined the influence of biofilm biomass (AFDM) on v_f and how it varied with the presence of bed forms (planform vs. bed form) using the Akaike Information Criterion (AIC) [*Akaike*, 1974] to select terms from a full analysis of covariance model (ANCOVA) including an interaction term. The full ANCOVA model includes three terms—flow heterogeneity as a categorical two-level factor, biofilm biomass as a continuous covariate, and the interaction term flow heterogeneity:biofilm biomass. A simpler two-way ANCOVA model would simultaneously test for two main effects: (i) differences between planform and bed form flume (a comparison of means) and (ii) the relationship of v_f with biofilm biomass (in the form of a linear regresssion). Statistical power for the test of flow heterogeneity effects is increased by the simultaneous adjustment for biofilm biomass effects and vice versa. In our case, we included an interaction term in addition to the main effects in the model, which allowed testing the null hypothesis of parallel slopes of v_f with biofilm biomass, or in other words, it addressed the question whether the relationship between v_f and biofilm biomass differed between planform and bed form flume. A significant interaction term points to different slopes between the flumes. A positive interaction term would suggest positive feedback, with bed forms and biofilms reinforcing each others' influence on v_f; a negative interaction term would suggest suppression of each factor's influence. An ANCOVA model of this type can be built stepwise to assess the influence of each of the three terms by p-values, or a likelihood-based, information-theoretic approach like the Akaike Information Criterion (AIC) can be used to aid in identifying the most parsimonious model, i.e., the one yielding the best overall fit relative to the number of parameters and data [*Burnham and Anderson,* 2002]. The model with the lowest AIC identifies the most parsimonious model, and competing models with AIC-values differing by less than 2 can be considered equivalent. We report both classical significance values and AIC values for the full and reduced models (where reduced models include only one or two terms—flow heterogeneity and biofilm biomass, both independently and together).

3. Results

3.1. Comparison of Hydrodynamic Conditions Between the Two Flume Treatments

Mean velocity was more heterogeneous in the bed form flume than in the planform flume (Figure 1). The spatial average of 80 ADV measurements over one bed form wavelength yielded lower average flow velocity for the planform flume compared to the bed form flume (Table 1). The reach-averaged Reynolds number was ~4300 in the planform flume and ~8300 in the bed form flume. The reach-averaged Froude number was ~0.09 in the planform flume and ~0.13 in the bed form flume. Turbulence was significantly higher in the bed form than the planform flume, as recorded by TKE and TI. Average TKE was more than 3 times greater in the

Table 2. Characterization of Flow and Transport Parameters Using Conservative Tracer Data in the Two Flumes Under Different Stages of Biofilm Growth[a]

	Planform Flume			Bed form Flume		
	Min Biofilm	Med Biofilm	Max Biofilm	Min Biofilm	Med Biofilm	Max Biofilm
A_s/A (−)	0.029 ± 0.002	0.071 ± 0.003	0.117 ± 0.005	0.029 ± 0.002	0.086 ± 0.003	0.112 ± 0.002
α_2 (h^{-1})	16.3 ± 1.7	9.6 ± 0.7	41.8 ± 2.4	18.5 ± 1.3	4.8 ± 0.3	9.1 ± 0.3
v (m h^{-1})	240.9 ± 0.3	261.1 ± 0.4	315.1 ± 1.3	214.4 ± 0.4	223.8 ± 0.4	240.4 ± 0.4
d (cm)	8.41 ± 0.59	7.75 ± 0.55	6.43 ± 0.45	9.44 ± 0.67	9.05 ± 0.64	8.42 ± 0.60
Da	0.38	0.73	0.21	0.30	1.26	0.73
Pe	130	140	376	103	90	99
D (m^2 h^{-1})	74.0 ± 1.5	74.5 ± 2.4	33.5 ± 2.8	82.9 ± 1.1	99.5 ± 2.0	96.7 ± 1.9

[a]Errors are ±1 SD estimated in the model.

bed form than the planform flume. Average TI was 1.2 times greater in the bed form than the planform flume. Both differences were significant at the $p < 0.05$ level. Velocity, TKE, and TI had much higher standard deviations over a bed form than over the same length of the planform streambed (Figure 1). More specifically, velocity, TKE, and TI were relatively homogeneous in the planform flume, the velocity generally increased
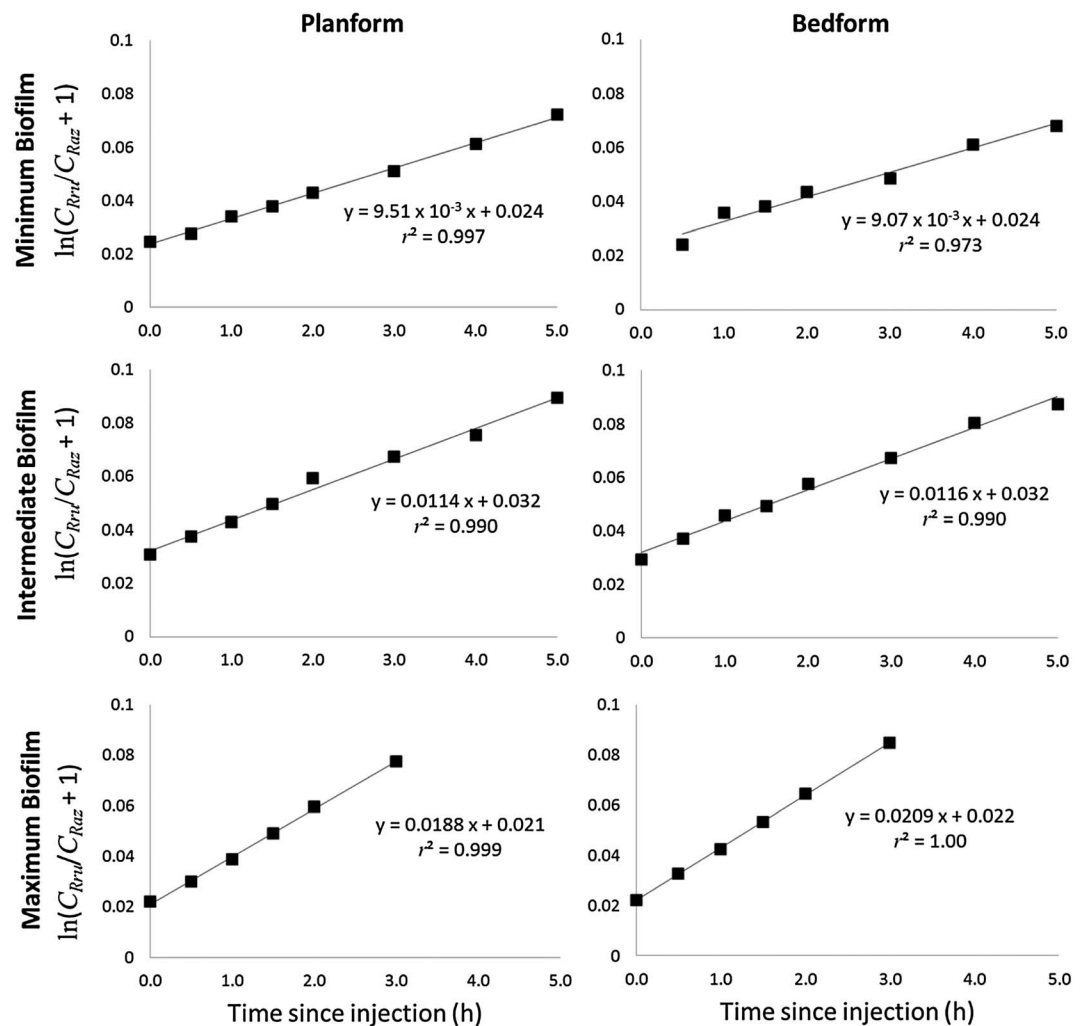

Figure 2. Temporal changes of the Rru to Raz ratio during the recirculation phase of the experiments. The different panels show data for the three levels of biofilm growth and for the two different bed forms. The increasing values of this ratio indicated a transformation of Raz (the oxidized form) to Rru (the reduced form). The slope of each line is $\frac{A_s}{A} k_{12}$ and is proportional to *ER*.
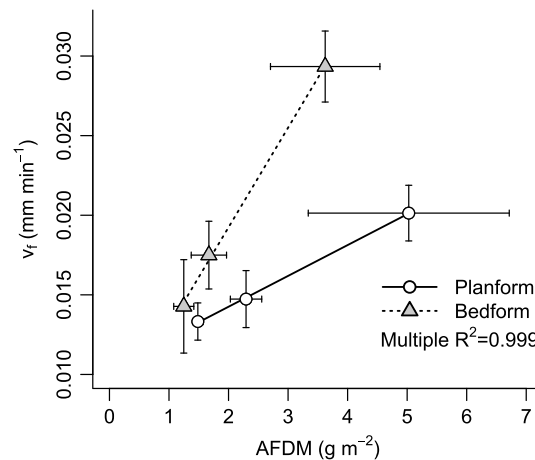
Figure 3. Biofilm respiration is greater in bed form than in planform flumes. Relationship between uptake velocity of Raz (v_f), which is proportional to ER, and biofilm biomass expressed as ash free dry mass (AFDM). The figure illustrates the full analysis of covariance (ANCOVA) model (Table 3) with separate slopes for the effect of biofilm biomass (AFDM) on v_f between the two flow heterogeneity treatments (planform vs. bed form flume) and thus a multiplicative interaction between the two predictors rather than a purely additive control on v_f.

along the upstream side and decreased along the downstream side of the bed forms. In the bed form flume, TKE peaked immediately downstream of the bed form crest, and TI was highest in the trough due to bed form-induced eddies that formed at the flow separation point at the bed form crest (Figure 1).

Conservative tracer data and model results (Table 2) indicated that transient storage size (i.e., A_s/A) in the two flume types was small, but it increased by 4 times as biofilm developed. Transient storage exchange rates (α_2) were fast but did not show any pattern with biofilm growth. The average Damköhler number, $Da = v\,(1 + A_s/A)/\alpha_2 L$, where L is the length of the flume, is 0.60 (range 0.21 – 1.26), indicating that the timescale of mass transfer between the water column and transient storage was approximately the same as the timescale of advection through the flume. Average velocities from multiple slug injections of NaCl solutions were 272 m h^{-1} for the planform flume and 226 m h^{-1} for the bed form flume (Table 2), but velocity differences were not significant at the $p < 0.05$ level. The velocities estimated from conservative solute tracer were smaller than the velocity means from the ADV. This was unexpected because the means from the ADV are spatial averages of slower, near-streambed velocities, while the velocities from the tracer are flux averages. Average depths were 7.53 ± 0.53 cm for the planform flume and 8.97 ± 0.63 cm for the bed form flume. Neither the average velocity nor average depth differs significantly at the $p < 0.05$ level between the planform and bed form flumes. Dispersion (D) was small relative to distance and velocity, resulting in an average Peclet number, $Pe = vL/D$, that was 157 (range 90 – 376). This indicated that transport was advection was at least 90 times faster than dispersion and supports the decision to ignore dispersion in the analysis of respiration.

3.2. Ecosystem Respiration

We observed gradual increases in the ratio between Rru and Raz during the recirculation phase of the experiments in the two flumes and under all stages of biofilm development (Figure 2). The relationships between the Rru:Raz ratio and time since injection stopped were all significant and allowed estimation of the v_f of Raz for all experiments as an indicator of ER. The v_f of Raz increased with biofilm biomass in both bed form treatments. Taken together, the respiration rate was more than twice as large in the flumes with maximum biofilm biomass than in the flumes with minimum biofilm biomass (Figure 3). In addition, ER increases were more pronounced in the bed form than in the planform flumes (Figure 3).

The standard set placed in ambient light had a very small Raz-to-Rru reaction rate (k_{12}). The rate during the three experiments was $8.7 \pm 4.2 \times 10^{-4}$ h^{-1} based on 2–3 samples in each of the three experiments. This rate is similar in magnitude to unfiltered water column rates observed in samples from Spanish streams [Haggerty et al., 2008]. This rate was ~100 times smaller than the Raz-to-Rru reaction rate in the flumes, and so concentrations and reaction rates in the flume were not adjusted for light effects.

3.3. Partitioning Effects of Flow Heterogeneity and Biofilm Biomass on ER

Compared to simpler models, the ANCOVA model including an interaction term was superior, according to the AIC (Table 3). The v_f of Raz is significantly influenced by biofilm biomass and bed form-induced flow heterogeneity. However, the effect of biofilm biomass—as captured by its slope with v_f—differs between the bed form and planform flumes, and therefore the model including the interaction term is parsimonious. While biofilm biomass alone can explain 41.5% of the variance of v_f combining biofilm biomass and bed form-induced flow heterogeneity as additive terms explained 77.1% of the variance. Importantly, further

Table 3. Identifying Controls on v_f of Raz by Analysis of Covariance (ANCOVA) Modeling[a]

				t-Values and Probabilities for Coefficients		
Model	Multiple r^2	AIC	edf	Flowhet	Bio	Flowhet:Bio
Flowhet	0.155	−59.5	2	$0.86^{p=0.44}$	–	–
Bio	0.415	−61.7	2	–	$1.68^{p=0.17}$	–
Flowhet + Bio	0.771	−65.4	3	$2.16^{p=0.12}$	$2.84^{p=0.07}$	–
Flowhet + Bio + Flowhet:Bio	0.999	−95.7	4	−6.48*	16.63**	20.91**

[a]The table gives significance values and AIC-values (including equivalent degrees of freedom corresponding to the number of free parameters) for the full ANCOVA model and various reduced models involving at least one of three possible linear terms: flow heterogeneity (*Flowhet*, categorical factor with 2 levels: planform and bed form), biofilm biomass (*Bio*, continuous covariate) and their interaction. v_f of Raz is the response variable for all models. Significance levels are written as superscripts above t-values (*** = $p < 0.001$, ** = $p < 0.01$, * = $p < 0.05$). Abbreviations: Flowhet = Flow heterogeneity, Bio = Biofilm biomass, AIC = Akaike Information Criterion, edf = equivalent degrees of freedom.

inclusion of an interaction term yields a model with a nearly perfect fit to the data (multiple $r^2 = 99\%$, $p < 0.001$). This indicates that flow heterogeneity and biofilm biomass interact synergistically to affect respiration nonlinearly. In other words, biofilm biomass has a greater effect (i.e., higher slope) on v_f in the presence of bed forms than on v_f in absence of bed forms.

4. Discussion

Results from this study using the Raz-Rru system as a metabolic tracer clearly showed that biofilm biomass and the presence of boundary roughness (impermeable bed forms in our study) increased respiration rates. Biofilm biomass and flow heterogeneity as induced by impermeable bed forms are highly significant factors in *ER*, and their interaction is also significant. Growth in biofilm biomass over 30 days increased the respiration, expressed by v_f, by a factor of 1.51 (i.e., +51%) in the planform flume and by a factor of 2.06 in the bed form flume. This compares to an increase in v_f from planform to bed form by a factor of 1.14 (i.e., +14%) at low biomass, and an increase in v_f from planform to bed form by a factor of 1.90 at highest biomass. (Surface area of the flume was not responsible for changes in v_f because the bed form flume had only 2 – 3% larger surface area than the planform flume.)

It is important to note that the magnitude of the biofilm-driven increase in *ER* and the bed form-driven increase in *ER* cannot be directly compared in a meaningful way. *ER* must be principally related to biofilm biomass, and a change in the physical environment alone cannot induce a change in *ER* by itself without respiratory activity of biofilms. However, our results demonstrated that the effect of biofilm biomass on *ER* is context specific and is modulated by the turbulence or flow heterogeneity of the environment. In fact, we observed a synergistic interaction between flow heterogeneity and biofilm biomass: greater flow heterogeneity leads to an increasingly stronger effect of biofilm biomass on v_f, i.e., flow heterogeneity facilitates increased metabolic activity of biofilms. Our results for respiration are consistent with those of *Singer et al.* [2010] for dissolved organic carbon (DOC) uptake obtained in the same flume setting. *Singer et al.* found that v_f for leaf leachate resembling natural dissolved organic matter was 1.28 times higher for the bed form flume than the planform flume. For additions of glucose, a more labile source of DOC, at various biofilm biomasses the same factor ranged between 1.61 and 1.83. The differences between bed form and planform flumes we found for v_f of Raz (1.14 – 1.90 times higher) are bracketing v_f of DOC, indicating a broad agreement between the variation in the DOC consumption-based estimates of v_f and the smart tracer respiration-based estimates of v_f. This suggests similar effects of bed form heterogeneity and biofilm biomass for the two rates and thus a potential coupling between biofilm DOC uptake and metabolism, expressed as respiration.

The value of the production-decay ratio, *P,* in equation (9) is uncertain but is needed for the calculation of the slope $\frac{A_s}{A}k_{12}$, and therefore for the calculation of v_f using the method adopted here. Any error in *P* feeds forward into an error in v_f. *Haggerty* [2013, equation (22) and following] showed that the slope $\frac{A_s}{A}k_{12}$ is moderately sensitive to the value of *P*. In our analyses, we assumed $P = 1$. We re-ran the calculations of v_f for $P = 0.7$ (30% decrease). We found that the values of v_f changed by a factor of 0.715 ± 0.002. That is, all of the values of v_f changed by almost exactly the same amount. Therefore, uncertainty in *P* generates proportional

uncertainty in the absolute value of v_f, but does not generate uncertainty in the relative values of v_f that are calculated with the same P. Therefore, the conclusions about how ER changes as a function of flow heterogeneity and biofilm growth are unaffected by uncertainty in P.

The observed increases in respiration with increases in biofilm biomass can be explained by the increase in cells that are respiring. Respiration may also change due to differences in community structure between different flow conditions and by succession over the period of the experiments. Furthermore, transient storage associated with biofilm biomass growth may further increase ER. *Battin et al.* [2003] showed that biofilms constitute a "living zone of transient storage", documenting that biofilm growth increased the volume of transient storage by a factor of approximately 4 in flume mesocosm experiments. In our experiments, biofilm growth increased the volume of transient storage by a similar factor. The volume of transient storage was 4.03 ± 0.33 times larger at 30 days than at 0 days in the planform flume, and 3.86 ± 0.28 times larger at 30 days than at 0 days in the bed form flume. *Bottacin-Busolin et al.* [2009] also found, in the same flumes, that biofilms and bed forms increased transient storage. *Battin et al.* [2003] hypothesized that biofilm streamers and other structures produced long-lived eddies that stored solutes, increasing their availability and interaction with the microbes. This may enhance the metabolic activity of the biofilms, resulting in higher rates of respiration. The fact that the size of transient storage in the experiments varied more with biofilm biomass than with bed form type further suports this explanation. The effect of transient storage zone size on respiration has also been reported in studies at stream reach scale [*Mulholland et al.*, 2001]. These common findings at different scales (i.e., within biofilms or in stream reaches) evidence the relevance of transient storage as a factor controlling respiration in stream ecosystems.

Our results clearly show that both changes in flow and biology influence ER, and that changes in flow and biology interact to influence ER. Further research into the physics and ecology of hydrodynamic controls, changes in biofilm structure, and feedbacks between hydrodynamics and biofilm structure should prove useful in understanding ER and other biogeochemical processes. In particular, detailed experimental study is needed to understand the mechanics of the feedback mechanisms and interactions.

5. Conclusions

The results of the flume study presented here support the hypothesis that ecosystem respiration (ER) increases with flow heterogeneity (turbulence) caused by bed forms across a range of biofilm conditions. Our experiments using the resazurin-to-resorufin (Raz-to-Rru) proxy for respiration in streamside flumes with natural water and a single layer of gravel (median diameter of 9.2 mm) produced ER (measured as uptake velocities, v_f) that increased with biofilm biomass and presence of bed forms. These factors interact, meaning that biofilm biomass appears to generate more respiration in the presence of bed forms than in the absence of bed forms. Furthermore, biofilms on the surface of a single layer of gravel increased transient storage in the flumes by a factor of approximately 4, regardless of bed forms.

References

Acuña, V., A. Giorgi, I. Muñoz, U. Uehlinger, and S. Sabater (2004), Flow extremes and benthic organic matter shape the metabolism of a headwater Mediterranean stream, *Freshwater Biol.*, 49, 960–971.

Akaike, H. (1974), A new look at the statistical model identification, *IEEE Trans. Autom. Control.*, 19(6), 716–723, doi:10.1109/TAC.1974.1100705.

Argerich, A., R. Haggerty, E. Martí, F. Sabater, and J. Zarnetske (2011), Quantification of metabolically active transient storage (MATS) in two reaches with contrasting transient storage and ecosystem respiration, *J. Geophys. Res.*, 116, G03034, doi:10.1029/2010JG001379.

Battin, T. J. (1999), Hydrologic flow paths control dissolved organic carbon fluxes and metabolism in an Alpine stream hyporheic zone, *Water Resour. Res.*, 35(10), 3159–3169, doi:10.1029/1999WR900144.

Battin, T. J., L. A. Kaplan, J. D. Newbold, and S. P. Hendricks (2003), Contributions of microbial biofilms to ecosystem processes in stream mesocosms, *Nature*, 426, 439–442.

Battin, T. J., S. Luyssaert, L. A. Kaplan, A. K. Aufdenkampe, A. Richter, and L. J. Tranvik (2009), The boundless carbon cycle, *Nat. Geosci.*, 2, 598–600.

Bencala, K. E., and R. A. Walters (1983), Simulation of solute transport in a mountain pool-and-riffle stream: A transient storage model, *Water Resour. Res.*, 19(3), 718–724, doi:10.1029/WR019i003p00718.

Bernot, M. J., et al. (2010), Inter-regional comparison of land-use effects on stream metabolism, *Freshwater Biol.*, 55, 1874–1890, doi:10.1111/j.1365-2427.2010.02422.x.

Bottacin-Busolin, A., G. Singer, M. Zaramella, T. J. Battin, and A. Marion (2009), Effects of streambed morphology and biofilm growth on the transient storage of solutes, *Environ. Sci. Technol.*, 43(19), 7337–7342.

Bradshaw, P. (1971), *An Introduction to Turbulence and its Measurement*, 232 pp., Pergamon Press, New York.

Burnham, K. P., and D. R. Anderson (2002), *Model Selection and Multimodel Interference: A Practical Information-Theoretic Approach*, Springer, New York.

Cardinale, B. J., M. A. Palmer, C. M. Swan, S. Brooks, and N. L. Poff (2002), The influence of substrate heterogeneity on biofilm metabolism in a stream ecosystem, *Ecology*, *83*(2), 412–422, doi:10.2307/2680024.

Cole, J. J., et al. (2007), Plumbing the global carbon cycle: Integrating inland waters into the terrestrial carbon budget, *Ecosystems*, *10*(1), 171–184, doi:10.1007/s10021-006-9013-8.

Dade, W. B., A. J. Hogg, and B. P. Boudreau (2001), Physics of flow above the sediment-water interface, in *The Benthic Boundary Layer*, edited by B. P. Boudreau and B. B. Jorgensen, pp. 4–43, Oxford Univ. Press, Oxford, U. K.

Demars, B. O. L., J. R. Manson, J. S. Ólafsson, G. M. Gíslason, and N. Friberg (2011), Stream hydraulics and temperature determine the metabolism of geothermal Icelandic streams, *Knowl. Manage. Aquat. Ecosyst.*, *402*, doi:10.1051/kmae/2011046.

Fellows, C. S., H. M. Valett, and C. N. Dahm (2001), Whole-stream metabolism in two montane streams: Contribution of the hyporheic zone, *Limnol. Oceanogr.*, *46*(3), 523–531.

Fuss, C., and L. Smock (1996), Spatial and temporal variation of microbial respiration rates in a blackwater stream, *Freshwater Biol.*, *36*(2), 339–349.

González-Pinzón, R., R. Haggerty, and D. D. Myrold (2012), Measuring aerobic respiration in stream ecosystems using the resazurin-resorufin system, *J. Geophys. Res.*, *117*, G00N06, doi:10.1029/2012JG001965.

Gordon, N. D., T. A. McMahon, B. L. Finlayson, C. J. Gippel, and R. J. Nathan (2004), *Stream Hydrology: An Introduction for Ecologists,* 2nd ed., 429 pp., John Wiley, Chichester, U. K.

Haggerty, R. (2013), Analytical solution and simplified analysis of coupled parent-daughter steady-state transport with multirate mass transfer, *Water Resour. Res.*, *49*, 635–639, doi:10.1029/2012WR012821.

Haggerty, R., and P. Reeves (2002), *STAMMT-L Version 1.0 User's Manual*, 76 pp., Sandia Natl. Lab., Albuquerque, N. M.

Haggerty, R., A. Argerich, and E. Martí (2008), Development of a "smart" tracer for the assessment of microbiological activity and sediment-water interaction in natural waters: The resazurin-resorufin system, *Water Resour. Res.*, *44*, W00D01, doi:10.1029/2007WR006670.

Haggerty, R., E. Martí, A. Argerich, D. von Schiller, and N. Grimm (2009), Resazurin as a "smart" tracer for quantifying metabolically active transient storage in stream ecosystems, *J. Geophys. Res.*, *114*, G03014, doi:10.1029/2008JG000942.

Hoellein, T. J., J. L. Tank, E. J. Rosi-Marshall, S. A. Entrekin, and G. A. Lamberti (2007), Controls on spatial and temporal variation of nutrient uptake in three Michigan headwater streams, *Limnol. Oceanogr.*, *52*(5), 1964–1977.

Ingendahl, D., D. Borchardt, N. Saenger, and P. Reichert (2009), Vertical hydraulic exchange and the contribution of hyporheic community respiration to whole ecosystem respiration in the River Lahn (Germany), *Aquat. Sci.*, *71*, 399–410, doi:10.1007/s00027-009-0116-0.

Inoue, T., and Y. Nakamura (2011), Effects of hydrodynamic conditions on DO transfer at a rough sediment surface, *J. Environ. Eng.*, *137*, 28–37.

Jones, J. B., Jr., S. G. Fisher, and N. B. Grimm (1995), Vertical hydrologic exchange and ecosystem metabolism in a Sonoran Desert stream, *Ecology*, *76*(3), 942–952.

Mulholland, P. J., E. R. Marzolfl, J. R. Webster, D. R. Hart, and S. P. Hendricks (1997), Evidence that hyporheic zones increase heterotrophic metabolism and phosphorus uptake in forest streams, *Limnol. Oceanogr.*, *42*(3), 443–451.

Mulholland, P. J., et al. (2001), Inter-biome comparison of factors controlling stream metabolism, *Freshwater Biol.*, *46*, 1503–1517.

Mulholland, P. J., et al. (2009), Nitrate removal in stream ecosystems measured by 15 N addition experiments: Denitrification, *Limnol. Oceanogr.*, *54*(3), 666–680.

Naegeli, M. W., and U. Uehlinger (1997), Contribution of the hyporheic zone to ecosystem metabolism in a pre-alpine gravel-bed river, *J. North Am. Benthol. Soc.*, *16*(4), 794–804.

O'Connor, B. L., and M. Hondzo (2008), Dissolved oxygen transfer to sediments by sweep and eject motions in aquatic environments, *Limnol. Oceanogr.*, *53*, 566–578.

O'Connor, B. L., M. Hondzo, and J. W. Harvey (2009), Incorporating both physical and kinetic limitations in quantifying dissolved oxygen flux to aquatic sediments, *J. Environ. Eng.*, *135*(12), 1304–1314.

O'Connor, B. L., J. W. Harvey, and L. E. McPhillips (2012), Thresholds of flow-induced bed disturbances and their effects on stream metabolism in an agricultural river, *Water Resour. Res.*, *48*, W08504, doi:10.1029/2011wr011488.

O'Connor, D. J. (1988), Models of sorptive toxic substances in freshwater systems. I: Basic equations, *J. Environ. Eng.*, *114*(3), 507–532.

Perkins, D. M., G. Yvon-Durocher, B. O. Demars, J. Reiss, D. E. Pichler, N. Friberg, M. Trimmer, and G. Woodward (2012), Consistent temperature dependence of respiration across ecosystems contrasting in thermal history, *Global Change Biol.*, *18*, 1300–1311.

R-Development-Core-Team (2010), *R: A Language and Environment for Statistical Computing*, R Foundation for Statistical Computing, Vienna, Austria. [Available at http://www.R-project.org.]

Runkel, R. L. (1998), *One-Dimensional Transport With Inflow and Storage (OTIS): A Solute Transport Model for Streams and Rivers*, U.S. Geol. Surv., Denver, Colo.

Singer, G., K. Besemer, P. Schmitt-Kopplin, I. Hödl, and T. J. Battin (2010), Physical heterogeneity increases biofilm resource use and its molecular diversity in stream mesocosms, *PLoS One*, *5*(4), e9988, doi:10.1371/journal.pone.0009988.

Sinsabaugh, R. L. (1997), Large-scale trends for stream benthic respiration, *J. North Am. Benthol. Soc.*, *16*(1), 119–122.

Stream Solute Workshop (SSW) (1990), Concepts and methods for assessing solute dynamics in stream ecosystems, *J. North Am. Benthol. Soc.*, *9*(2), 95–119.

Tranvik, L. J., et al. (2009), Lakes and reservoirs as regulators of carbon cycling and climate, *Limnol. Oceanogr.*, *54*, 2298–2314, doi:10.4319/lo.2009.54.6_part_2.2298.

Yvon-Durocher, G., et al. (2012), Reconciling the temperature dependence of respiration across timescales and ecosystem types, *Nature*, *487*(7408), 472–476, doi:10.1038/nature11205.